Zhao, C, Xing, X, Guo, J, Shi, Z, Zhou, Y, Ren, X and Yang, Q

Micro-properties of (Nb,M)C carbide (M = V, Mo, W and Cr) and precipitation behavior of (Nb,V)C in carbide reinforced coating

Micro-properties of (Nb,M)C carbide (M¼V, Mo, W and Cr) andprecipitation behavior of (Nb,V)C in carbide reinforced coating

Changchun Zhao[a], Xiaolei Xing[a], b, Jing Guo[c], Zhijun Shi[a], Yefei Zhou[a, b, **], Xuejun Ren[d], Qingxiang Yang
[a] State Key Laboratory of Metastable Materials Science & Technology, Yanshan University, Qinhuangdao 066004, PR China
[b] College of Mechanical Engineering, Yanshan University, Qinhuangdao 066004, PR China
[c] College of Metallurgy and Energy, North China University of Science and Technology, Hebei Key Laboratory of Modern Metallurgy Technology, Tangshan, 063009, PR China
[d] School of Engineering, Liverpool John Moores University, Liverpool L3 3AF, UK

Abstract

In this work, the Micro-properties such as stability, mechanical parameter and bonding structures of (Nb,M)C carbides (M ¼ V, Mo, W and Cr) were calculated. And the misfit and interfacial combination between (Nb,M)C carbides and Fe matrix were investigated by first principles calculation. The precipitation behavior of (Nb,V)C carbides were studied. The element V distribution of the carbide in the coatings were analyzed by experiments. The calculation results show that, in the (Nb,M)C carbides, the lattice constant and formation energy of Nb0.75V0.25C carbide are the smallest, and its hardness and brittleness are the largest. According to bonding analysis, Nb-C covalent bonds are the main factor for its high hardness in Nb0.75V0.25C carbide. The combination between carbide and Fe matrix is improved from the results of misfit and adhesion work. Based on the diagrams of the hardfacing alloys with different V contents, the fraction of MC carbides is increased with increase of V contents, and VC carbide can precipitate when V content is high enough. It indicates that element V can be introduced into NbC carbide from the chemical elements analysis experiments.

1. Introduction

Niobium carbide (NbC) reinforced Fe-based composite coatings has been widely used as strengthen material in surface modification of iron based materials for its excellent characteristics, such as high hardness, outstanding wear resistance and advantage of price [1e3]. In recent years, multiple reinforced particles reinforced coatings have been produced by researchers to further improve the wear resistance of coatings [4e6]. Cao et al. [7,8] report a highvanadium hierarchical coating prepared on the surface of nodular cast iron substrate by a low-cost plasma transferred arc (PTA) surface alloying process. They observed that submicron sized granular (V-Ti-Nb-Cr-Mo) composite carbides precipitate on top of intermediate melted zone. Dash et al. [9] prepared WC-TiC composite. with six different values of TiC in the range 1e15 wt% by arc plasma (Ar) melting and found that the hardness of composites are improved and reach a maximum value of 3650 ± 75 VHN due to the presence of phases such as TiC, TiC0.981/TiC1-x and TiWC2/(Ti,W)C. Wang et al. [10] fabricated TiC-VC-Mo2C carbides reinforced Febased hardfacing layers by shielded manual arc welding (SMAW). The hardfacing layer with good cracking resistance and high hardness could be obtained when the amounts of graphite, FeeTi, FeeV and FeeMo were well controlled. Li et al. [11] investigated the precipitate behavior of (Ti, Nb)C particles in Fe-based composite coatings with different Ti/Nb atomic ratio and found that the hardness and wear resistance of the coating is significantly improved.

Our previous studies [12] have investigated the strengthening mechanism of (Nb, Ti)C carbide composite coatings, and we found that the addition of Ti can increase the hardness of carbides, reduce the mismatch between them and the matrix, and promote the formation of primary granular carbides, which are beneficial to the wear resistance of coating. Elements V, Mo, W and Cr are also MC type carbide forming ones, and their formation ability are weaker than that of Nb. So they may form together

with NbC and act as the shell of multiple carbide [7,8], and these multiple carbide may strongly affect the interfacial combination between carbides and Fe matrix.

To learn the strengthening mechanism of multiple carbide reinforced coating, the micro-properties of the multiple carbide and the interfacial combination between carbide and matrix are needed. However, it is difficult to make it clear only by experiments due to the changes of chemical composition and crystal orientations [13] of different carbides. First-principles calculation based on density functional theory (DFT) has been widely applied in the structures and properties investigation [14e20]. Jang et al. [21] investigated the stability of TiC carbide doped by Nb, V, Mo and Cr and indicated that (Ti, Mo)C and (Ti, W)C carbides are more energetically stable and lower misfit strain between them and ferrite matrix. Kavitha et al. [22] investigated structural, electronic, mechanical and superconducting properties of CrC and MoC carbides with different crystal structures and found thatWC structure is the most stable structure at normal pressure. Yang et al. [23,24] researched the interfacial combination of NbC (111)/NbN (111) interface and indicated that stacking sequence plays an important role on the interfacial stability. It seems that first-principles calculation is an effective method to investigate the stability, mechanical properties and interfacial combination of materials.

In this work, the formation energy, hardness, brittleness and bonding structures of (Nb,M)C carbides were calculated. The misfit and interfacial combination between (Nb,M)C carbides and Fe matrix were investigated. The precipitation behavior of (Nb,V)C carbides with different V contents were studied. Subsequently, the element V distribution of the carbide in the coating was analyzed.

2. Experimental methods and computational details

2.1. Experimental methods

The Fe matrix NbC composites coatings were produced by fluxcored arc welding (FCAW) hardfacing technology. The core of fluxcored wire was made of different raw materials, such as ferroniobium, The phase identification of the coating was carried out on X-ray diffraction (XRD; Rigaku D/Max-2500/PC) with CuKa operating at 40 kV. The hardfacing specimen was etched with 4% nitric acid alcohol. The microstructure of the coating was observed with a scanning electron microscope (FE-SEM; HITACHI S-4800) equipped with an energy-dispersive spectroscopy (EDS; E-MAX) and a transmission electron microscopy (TEM; JEM-2010).ferrochromium, ferromanganese, ferrovanadium, ferrosilicon and graphite powder, and the shell of flux-cored wire was made up of low-carbon steel strip of H08A. The flux-cored wires were deposited on Q235 low-carbon steel plates. The details of hardfacing process and flux-cored wire manufacturing were based on our previous work [25]. The compositions of the coatings with 0.66 wt% V addition are listed in Table 1.

The phase identification of the coating was carried out on X-ray diffraction (XRD; Rigaku D/Max-2500/PC) with CuKa operating at 40 kV. The hardfacing specimen was etched with 4% nitric acid alcohol. The microstructure of the coating was observed with a scanning electron microscope (FE-SEM; HITACHI S-4800) equipped with an energy-dispersive spectroscopy (EDS; E-MAX) and a transmission electron microscopy (TEM; JEM-2010).

2.2. Computational details

First-principles calculations based on density functional theory (DFT) with ultrasoft pseudopotentials were used to evaluate some mechanical properties of (Nb,M)C and interfacial combination of (Nb,M)C/Fe interface. The calculations were performed by using Cambridge Sequential Total Energy Package (CASTEP) [26]. The generalized gradient approximation (GGA) with Perdew-Burke-Ernzerhof (PBE) functional was employed as exchange-correlation energy [27]. The mechanical parameters of (Nb,M)C were calculated by the Voigt-Reuss-Hill (VRH) approximation method [28]. On the basis of convergence tests, plane-wave cutoff energy was set at 540eV and Brillouin zone sampling was set at 16 x 16 x 16 Monkhorst-Pack mesh for bulk calculation, and 380eV cutoff energy

and 8 x 8 x 1 Monkhorst-Pack mesh for interface calculation. The numbers of (Nb,M)C surface layers are 13 and the numbers of Fe surface layers are 5. The 12 Å vacuum space along the c-axis was used during interface calculation to eliminate the long interactions from periodic boundary condition calculation. The energy, the maximum force and maximum displacement were set as 1 x 10^{-5} eV/atom, 0.01 eV/Å and 1 x10^{-3} Å for the convergence tolerances, respectively.

The phase diagrams of the coatings with different V contents were calculated by Thermo-Calc software. The databases is TCFE7. The calculated temperature is from 2000K to 1000 K and the step is 10 K. The calculation elements contents were the same with the compositions of the V-1 coating (without V element).

3. Effect of elements V, Mo, W and Cr on stability, hardness and interfacial combination of (Nb,M)C carbide

3.1. Mechanical parameters and formation energy of (Nb,M)C

The structures of NbC and (Nb,M)C carbides are shown in Fig. 1. They are face-centered cube with FM-3M space group, in which, each carbide cell contains eight atoms. In order to obtain results of different (Nb,M)C carbides for comparison, one of the Nb atoms in NbC carbide was substituted by V, Mo, W and Cr atoms, respectively, which maybe expressed as Nb0.75M0.25C to do calculation. The elastic modulus (E) and poisson's ratio (n) of Nb0.75M0.25C carbides can be estimated as follows:

$$E = 9BG/(3B + G) \quad (1)$$

$$\nu = (3B - 2G)/2(3B + G) \quad (2)$$

where B and G are the bulk modulus and shear modulus, respectively, which can be given directly by calculating.

The formation energy (Efor) can be get by Eq. (3) [21]:

$$E_{for}^{(Nb,M)C} = \frac{1}{m+n+l}\left(E_{(Nb,M)C}^{total} - mE_{Nb}^{bulk} - nE_{M}^{bulk} - lE_{C}^{graphite}\right) \quad (3)$$

where $E_{(Nb,M)C}^{total}$ is the total energy of Nb0.75M0.25C carbide; E_{Nb}^{bbc} and $E_{C}^{graphite}$ are the energies of one atomin body-centered (bbc) Nb and graphite C, respectively; Ebulk M are the energies of one atom in body-centered (bbc) V, Mo, W and Cr, respectively; m, n and l are the numbers of Nb atoms, M atoms and C atoms in one Nb0.75M0.25C unit, respectively. E_{M}^{bulk} are the energies of one atom in body centered (bbc) V, Mo, W and Cr, respectively; m, n and l are the numbers of Nb atoms, M atoms and C atoms in one Nb0.75M0.25C unit, respectively. The calculated results of Nb0.75M0.25C are listed in Table 2, which were compared with other previous works [21,29-31]. The lattice constants of Nb0.75M0.25C carbides are decreased compared with NbC, and Nb0.75V0.25C carbide presents the minimum lattice constants among Nb0.75M0.25C carbides. As can be seen in Table 2, the replacement of Nb atom by V, Mo,Wand Cr atoms can increase the formation energy of the carbides, in which, formation energy of Nb0.75V0.25C carbide is the smallest. It indicates that, the stability of V atom in (Nb,M)C carbides is the largest. The elastic constants (Cij) were calculated by Voigt-Reuss-Hill approximation to estimate the mechanical stability of Nb0.75M0.25C carbides, which are listed in Table 3. It can be seen that all the Nb0.75M0.25C carbides obey the following relationship: C11 > 0; C33 > 0; C44 > 0; C66 > 0; C11-C12>0; C11+C33-2C13 > 0;

2(C11+C12)+C33+4C13 > 0, which indicates that the replacement of Nb atom by V, Mo, W and Cr atoms in (Nb,M)C is mechanically stable.

3.2. Theoretical hardness and bonding structure of (Nb,M)C

Hardness of carbide is an important factor for the wear resistance of the carbide reinforced coatings. Therefore, the hardness of Nb0.75M0.25C affected by elements V, Mo, W and Cr should be evaluated. The theoretical hardness of Nb0.75M0.25C carbides can be calculated from bulk modulus B and shear modulus G and they have the following relationship [32]:

$$Hv = 0.92K^{1.137}G^{0.708} \quad (4)$$

$$K = G/B \quad (5)$$

where Hv are the theoretical hardness; K is the Pugh's modulus ratio. The calculated results are shown in Fig. 2. The calculated hardness of NbC in this work is 24.54 GPa, and it is matched well with other previous work (24.1 GPa, 24.5 GPa) [30]. Compared with NbC, the hardness of Nb0.75V0.25C and Nb0.75W0.25C are obviously increased to 27.55 GPa and 26.26 GPa, respectively. However, those of Nb0.75Mo0.25C and Nb0.75Cr0.25C are decreased to 23.86 GPa and 23.06Gpa, respectively. It means that, element V can greatly increase the hardness of the carbide. The Pugh's modulus ratio 'K' [33] can be used to describe the brittleness of carbides. From Fig. 2, all the carbide equipped with brittle character because their 'K' are bigger than 0.571, and compared with NbC, the brittleness of Nb0.75V0.25C, Nb0.75W0.25C and Nb0.75Cr0.25C carbide are increased and that of Nb0.75Mo0.25C carbide is decreased.

From calculated hardness results, the hardness of carbide, which is closely related to its bonds structure, can be strongly affected by elements V, Mo,Wand Cr. It is necessary to investigate the bonding situation of carbides, to learn the effects of these elements on the hardness of the carbide. Fig. 3 is the partial density of states (PDOS) of Nb0.75Mo0.25C carbides. From it, the N(EF) of all Nb0.75M0.25C carbides are larger than 0, which shows that all of the Nb0.75M0.25C carbides present metallic character. The metallicity of Nb0.75M0.25C carbides can be calculated as follows [34]:

$$f_m = \frac{n_m}{n_e} = \frac{k_B T D_f}{n_e} = \frac{0.026 D_f}{n_e} = \frac{0.026 D_f V_{cell}}{N} \quad (6)$$

where nm and ne represent the thermal excited electrons and valence electron density of carbides, respectively; kB, T and Df denote the Boltzmann constant, temperature and DOS value of carbides at fermi level, respectively; Vcell and N are the volume of carbides and total number of the valance electrons of the carbides, respectively. The metallicity of Nb0.75M0.25C carbides were calculated and listed in Table 4. As can be seen, the metallicity of Nb0.75M0.25C carbides are bigger than that of NbC. Their metallicity are decreased in the following order: Nb0.75V0.25C > Nb0.75Cr0.25C > Nb0.75Mo0.25C > Nb0.75W0.25C > NbC. And overlapped orbits can be seen clearly in all carbides, which indicates that the Nb-C, V-C, Mo-C, W-C and Cr-C covalent bonds are formed in the carbides.

The information of ionicity and electron transfer of atoms in these carbides, which are very helpful to study the contribution of V, Mo, W and Cr atoms to the hardness of Nb0.75M0.25C carbides, should be learned. The plane (002), which pass through Nb, V, Mo, W, Cr and C atoms, was selected as the plane for plots of charge density differences and charge densities. They are shown in Fig. 4 and Fig. 5, respectively. From Fig. 4, charge depletion region of Nb,

V, Mo, W and Cr atoms and charge obtain region of C atoms can be found, which indicates the formation of ionic bonds between metal atoms and carbon. The Mulliken populations of Nb0.75M0.25C carbides, which can help to analyze the detail of charge transfer, are listed in Table 5. As can be seen from the atomic populations, charges transfer in Nb0.75V0.25C from Nb atom to C atom are less than that in other carbides, and the charges transfer from V atom to C atom are much more than that of metal atoms in other carbides. The directional spatial distribution of electrons between Nb and C atoms can be seen in Fig. 5, which means the formation of Nb-C covalent bonds. Besides, the directional spatial distribution of electrons can also be observed between Mo and C atoms orWand C atoms. Strong directional covalent bonds are considered to be dominant factor for the hardness of material [32]. Therefore, it is helpful to study the covalent bonds in carbides to understand the hardness changes of carbides affected by elements V, Mo,Wand Cr.

The bond populations of Nb0.75M0.25C carbides were also calculated and the bond populations of Nb-C bonds (away and near the M-C bonds) and M-C bonds are listed in Table 5. From it, the strong Nb-C covalent bonds can be observed in Nb0.75V0.25C carbide. And the strong W-C covalent bonds can be observed in Nb0.75W0.25C carbide. Obviously, strong Nb-C covalent bonds and W-C covalent bonds are the main factors for the high hardness of Nb0.75V0.25C and Nb0.75W0.25C carbide, respectively. Although strong Nb-C covalent bonds can also be found in Nb0.75Cr0.25C, the low strength of Cr-C bond in MC type carbide may be the reason for the hardness decrease of Nb0.75Cr0.25C carbide [22].

3.3. Interfacial combination of (Nb,M)C with Fe matrix

The lattice parameter of carbides are decreased caused by the introduction of V, Mo, W and Cr atoms, and the lattice misfit between them and matrix may also decreased. Some previous works [35] show that the low misfit can decrease elastic strain energy between precipitates and the matrix. Therefore the misfit between Nb0.75M0.25C carbides and Fe matrix should be studied. The crystallographic relationship between MC type carbide and a-Fe is always described by Baker-Nutting relationship [36]:

$$(100)_a \| (100)_{(Nb,M)C},\quad [010]_{aFe} \| [011]_{(Nb,M)C}$$

Therefore the lattice misfit between Nb0.75M0.25C carbides and a-Fe can be get:

$$\delta = \left(a_{carbide} - \sqrt{2}a_{aFe}\right) / a_{carbide} \quad (7)$$

where δ is the lattice misfit between a-Fe and Nb0.75M0.25C carbides; $a_{carbide}$ and $a_{\alpha Fe}$ are the calculated lattice parameter of Nb0.75M0.25C and a-Fe, respectively.

It can be learned from Eq. (7) that, the smaller lattice parameters of carbide is, the lower d is. Compared with NbC, the lattice parameters of Nb0.75M0.25C are decreased, therefore the replacement of V, Mo,Wand Cr in NbC carbide can decrease the misfit between carbide and matrix. The lattice parameter of Nb0.75V0.25C carbide is 4.419 Å, which is the smallest parameter among Nb0.75M0.25C carbides. In this work, the lattice parameter of NbC and a-Fe are 4.46 Å, and 2.87 Å, respectively. The d between NbC and a-Fe is 8.9%, and that of Nb0.75V0.25C is decreased to 8.1%.

The interfacial combination of Nb0.75M0.25C carbide with Fe matrix may also be affected by the introduction of elements V, Mo,W and Cr. The interfacial models based on Baker-Nutting relationship were built, which are shown in Fig. 6. The adhesion work (Wad) can reflect the binding strength of the interfaces and it can be obtained by Eq. (7) [37,38]:

$$W_{ad} = \left(E_{\alpha Fe} + E_{(Nb,M)C} - E_{\alpha Fe/(Nb,M)C}\right)/A \quad (8)$$

where E_{aFe} and $E_{(Nb,M)C}$ are the total energies of Fe and Nb0.75M0.25C relaxed, respectively; $E_{aFe/(Nb;M)C}$ is the total energy of the interface system; A is the interface area. The Wad of the interfaces is listed in Table 6. It can be seen that the Wad of some models are negative, which indicates that separating the interface into two free surfaces is energy needed. The Wad of M-termination models are larger than that of C-termination models, which indicates that M-termination models are more stable. It is noteworthy that theWad of NbCrC-Fe interface are positive and larger than any other interfaces, which means that the NbCrCFe interface is most stable. Besides, the Wad of NbVC-Fe is only smaller than that of NbCrC-Fe and larger than the rest interfaces, which indicates that the NbVC-Fe interface is also stable. From the Wad, the stability order of C termination interface models is as following: NbCrC-Fe > NbVC-Fe > NbMoC-Fe > NbC-Fe > NbWC-Fe. And the stability order of M termination interface models is as following: NbCrC-Fe > NbVC-Fe > NbVC-Fe > NbC-Fe > NbMoC-Fe.

The interface distance (d) is also listed in Table 6. From Table 6, the d of M-termination models is larger than that of C-termination models, and the changes of d in M-termination models are also larger than that in C-termination models. The interface distance of Nb0.75Mo0.25C carbide with Fe in M-termination models is the smallest.

4. Effect of element V on precipitation behavior of the carbide

From the calculation results, compared with other Nb0.75M0.25C carbides, Nb0.75V0.25C has the lowest forming energy, the largest hardness, the smallest mismatch with the matrix, and the better stability (only worse than Nb0.75Cr0.25C) with matrix. Therefore, the element V is an ideal alloying element with NbC composite carbide. However, in the actual situation, the addition of elements in the coating is a complex process, that affects the other phases in the coating. Therefore, it is necessary to analyze the phase precipitation behavior and microstructure.

4.1. Effect of element V on the precipitation behavior of the carbide

Diagrams of the coatings with different V contents have been calculated, which are shown in Fig. 7. From Fig. 7, the precipitation temperature of MC carbide and g-Fe are slightly decreased with increase of V contents. However, the temperature gap between them are almost unchanged, which indicates that the amount of primary carbide and eutectic carbide will not be changed. The precipitation temperature and amount of M7C3 carbide are decreased. The content of MC is increased and it reaches the maximum value when V content is 0.6 wt%. It is noteworthy that, VC carbide begin to appear when V content is 0.8 wt%, and the amount of MC and M7C3 carbides are decreased. It can be known that the element V is introduced into MC and M7C3 carbide and it will precipitate in form of VC carbide when V content is high enough. Based on our previous work [39], M7C3 carbide was found to be of desquamation property during wear process which is bad for wear resistance. Therefore, the ideal result is that the amount of MC is increased and the amount of other carbides is decreased, so the proper addition of element V is about 0.6 wt%.

4.2. Microstructure of the carbides with V addition

The V content in V-1 coating is 0.66 wt%. The XRD result of V-1 coating is shown in Fig. 8, in which only g-Fe phase, a-Fe phase and MC type carbide peaks can be found. The

microstructures and elements mapping of V-1 coating are shown in Fig. 9. From it, the element V can be found in the carbides, and the element Cr is not introducing into carbide. To learn the details of element contents of the carbide, the contents of area 1 in carbide was tested by energy dispersive spectrometer and the results are listed in Table 7. From Table 7, the carbide are mainly composed of elements Nb, Ti, V and C. Although, the V content is less than other elements content, it may indicate that the element V could be introduced into NbC carbide. To investigate the crystal structures of carbide, the TEM micrograph of carbide and its selected area electron diffraction (SAED) patterns were conducted which are shown in Fig. 10. From Fig. 10 (b), the carbide has only one suit of electron diffraction pattern, which indicates that the element V could be introduced into NbC carbide with single crystal structure.

5. Conclusions

(1) The replacement of Nb atom by V, Mo, W and Cr atoms in Nb0.75M0.25C increase the formation energy of Nb0.75M0.25C carbide. In all Nb0.75M0.25C carbides, the formation energy of Nb0.75V0.25C carbide is the lowest, which indicates that, the stability of introducing V atom in Nb0.75M0.25C carbide is the best.
(2) The theoretical hardness of Nb0.75M0.25C carbide can be increased by introducing elements V and W. The Nb-C covalent bonds in Nb0.75V0.25C and W-C covalent bonds in Nb0.75W0.25C are the main factor for their high hardness, respectively.
(3) The misfit between a-Fe and carbides are decreased by the introduction of V, Mo, W and Cr atoms, and among them, Nb0.75Cr0.25C can mostly improve the interfacial combination. Besides, Nb0.75V0.25C can also improve the interfacial combination compared with NbC.
(4) Based on the diagrams with different V contents, the amount of MC carbides is increased with increase of V contents, and VC carbide will precipitate when V contents is high enough. And element V can be introduced into NbC carbide according to chemical elements analysis experiments.

Acknowledgement

The authors would like to express their gratitude for projects supported by the National Natural Science Foundation of China (No. 51471148, No.51771167 and No.51705447), Natural Science Foundation of Hebei Province (China) (E2017209180) and the Royal Society International Exchange Program.

References

[1] X.H. Wang, Z.D. Zou, S.Y. Qu, S.L. Song, Microstructure and wear properties of Fe-based hardfacing coating reinforced by TiC particles, J. Mater. Process. Technol. 168 (1) (2005) 89e94.
[2] R. Colaço, R. Vilar, Laser rapid-alloy prototyping for the development of wear resistant FeeCreC/NbC composite materials, J. Laser Appl. 15 (4) (2003) 267e272.
[3] N. Zhao, Y. Xu, W. Zhang, Z. Zhao, L. Zhong, Y. Fu, Gradually varying mechanical properties of in situ synthesized NbCeFe-graded composite coating, Mater. Sci. Technol. 33 (2) (2016) 220e226.
[4] A.K. Srivastava, K. Das, Microstructure and abrasive wear study of (Ti,W)Creinforced high-manganese austenitic steel matrix composite, Mater. Lett. 62 (24) (2008) 3947e3950.
[5] D. Ravnikar, N.B. Dahotre, J. Grum, Laser coating of aluminum alloy EN AW 6082-T651 with TiB2 and TiC: microstructure and mechanical properties, Appl. Surf. Sci. 282 (2013) 914e922.
[6] J. Jung, S. Kang, Sintered (Ti,W)C carbides, Scripta Mater. 56 (7) (2007)561e564.
[7] H. Cao, X. Dong, S. Chen, M. Dutka, Y. Pei, Microstructure evolutions of graded high-vanadium tool steel composite coating in-situ fabricated via atmospheric plasma beam alloying, J. Alloys Compd. 720 (2017) 169e181.
[8] H.T. Cao, X.P. Dong, A. Chabok, J.C. Rao, J.T.M. De Hosson, Y.T. Pei, Hard-yet tough high-vanadium hierarchical composite coating: microstructure and mechanical properties, Mater. Sci. Eng. A 736 (2018) 87e99.

[9] T. Dash, B.B. Nayak, Tungsten carbide e titanium carbide composite preparation by arc plasma melting and its characterization, Ceram. Int. 45 (2019) 4771e4780.
[10] X.H. Wang, F. Han, S.Y. Qu, Z.D. Zou, Microstructure of the Fe-based hardfacing layers reinforced by TiC-VC-Mo2C particles, Surf. Coating. Technol. 202 (8) (2008) 1502e1509.
[11] Q. Li, Y. Lei, H. Fu, Growth mechanism, distribution characteristics and reinforcing behavior of (Ti, Nb)C particle in laser cladded Fe-based composite coating, Appl. Surf. Sci. 316 (2014) 610e616.
[12] C. Zhao, Y. Zhou, X. Xing, S. Liu, X. Ren, Q. Yang, Precipitation stability and micro-property of (Nb, Ti)C carbides in MMC coating, J. Alloys Compd. 763 (2018) 670e678.
[13] Y. Kumashiro, A. Itoh, T. Kinoshita, M. Sobajima, The micro-Vickers hardness of TiC single crystals up to 1500 C, J. Mater. Sci. 12 (3) (1977) 595e601.
[14] Y. Ikeda, B. Grabowski, F. K€ormann, Ab initio phase stabilities and mechanical properties of multicomponent alloys: a comprehensive review for high entropy alloys and compositionally complex alloys, Mater. Char. 147 (2019)464e511.
[15] J. Xu, J. Cheng, S. Jiang, P. Munroe, Z.H. Xie, The influence of Ti additions on the mechanical and electrochemical behavior of b-Ta 5 Si 3 nanocrystalline coating, Appl. Surf. Sci. 419 (2017) 901e915.
[16] X.Y. Chong, Y.H. Jiang, R. Zhou, J. Feng, Electronic structure, mechanical and thermal properties of V-C binary compounds, RSC Adv. 4 (85) (2014) 44959e44971.
[17] Y.Z. Liu, Y.H. Jiang, F. Jing, Z. Rong, Elasticity, electronic properties and hardness of MoC investigated by first principles calculations, Phys. B Condens. Matter 419 (21) (2013) 45e50.
[18] Y. Jian, W. Yue, J. Huang, W. Wang, Y. Zheng, S. Chen, Z. Yue, First-principles calculations on interface structure and fracture characteristic of TiC/TiZrC nano-multilayer film based on virtual crystal approximation, J. Alloys Compd.
755 (2018) 211e223.
[19] X.Y. Chong, Y.H. Jiang, R. Zhou, J. Feng, Stability, chemical bonding behavior, elastic properties and lattice thermal conductivity of molybdenum and tungsten borides under hydrostatic pressure, Ceram. Int. 42 (2) (2016) 2117e2132.
[20] Y.Z. Liu, Y.H. Jiang, Z. Rong, F. Jing, First principles study the stability and mechanical properties of MC (M¼Ti, V, Zr, Nb, Hf and Ta) compounds, J. Alloys Compd. 582 (2) (2014) 500e504.
[21] J.H. Jang, C.H. Lee, Y.U. Heo, D.W. Suh, Stability of (Ti,M)C (M¼Nb, V, Mo and W) carbide in steels using first-principles calculations, Acta Mater. 60 (1) (2012) 208e217.
[22] M. Kavitha, G. Sudha Priyanga, R. Rajeswarapalanichamy, K. Iyakutti, Structural stability, electronic, mechanical and superconducting properties of CrC and MoC, Mater. Chem. Phys. 169 (2016) 71e81.
[23] J. Yang, J. Huang, D. Fan, S. Chen, First-principles investigation on the electronic property and bonding configuration of NbC (111)/NbN (111) interface, J. Alloys Compd. 689 (2016) 874e884.
[24] J. Yang, Z. Ye, J. Huang, S. Chen, Y. Zhao, First-principles calculations on
wetting interface between Ag-Cu-Ti filler metal and SiC ceramic: Ag (111)/SiC (111) interface and Ag (111)/TiC (111) interface, Appl. Surf. Sci. 462 (2018) 55e64.
[25] X. Yun, Y.F. Zhou, B. Zhao, X.L. Xing, J. Yang, Y.L. Yang, Q.X. Yang, Influence of nano-Y2O3 on wear resistance of hypereutectic FeeCreC hardfacing coating, Tribol. Lett. 58 (2) (2015) 23.
[26] D. Vanderbilt, Soft self-consistent pseudopotentials in a generalized eigenvalue formalism, Phys. Rev. B 41 (11) (1990) 7892e7895.
[27] J.P. Perdew, E.R. McMullen, A. Zunger, Density-functional theory of the correlation energy in atoms and ions: a simple analytic model and a challenge, Phys. Rev. A 23 (6) (1981) 2785e2789.
[28] W. Boas, Physical properties of crystals, their representation by tensors and matrices, J. Mech. Phys. Solid. 6 (4) (1958) 328e329.
[29] A.M. Nartowski, I.P. Parkin, M. Mackenzie, A.J. Craven, Solid state metathesis: synthesis of metal carbides from metal oxides, J. Mater. Chem. 11 (12) (2001) 3116e3119.
[30] L. Wu, Y. Wang, Z. Yan, J. Zhang, F. Xiao, B. Liao, The phase stability and mechanical properties of NbeC system: using first-principles calculations and nano-indentation, J. Alloys Compd. 561 (2013) 220e227.
[31] A. Teresiak, H. Kubsch, X-ray investigations of high energy ball milled transition metal carbides, Nanostruct. Mater. 6 (5) (1995) 671e674.

[32] Y. Tian, B. Xu, Z. Zhao, Microscopic theory of hardness and design of novel superhard crystals, Int. J. Refract. Metals Hard Mater. 33 (2012) 93e106.
[33] S.F. Pugh, XCII. Relations between the elastic moduli and the plastic properties of polycrystalline pure metals, Phil. Mag. 45 (367) (2009) 823e843.
[34] Y. Li, Y. Gao, B. Xiao, T. Min, Y. Yang, S. Ma, D. Yi, The electronic, mechanical properties and theoretical hardness of chromium carbides by first-principles calculations, J. Alloys Compd. 509 (17) (2011) 5242e5249.
[35] S. Jiang, H. Wang, Y. Wu, X. Liu, H. Chen, M. Yao, B. Gault, D. Ponge, D. Raabe, A. Hirata, M. Chen, Y. Wang, Z. Lu, Ultrastrong steel via minimal lattice misfit and high-density nanoprecipitation, Nature 544 (7651) (2017) 460e464.
[36] M. Charleux, W.J. Poole, M. Militzer, A. Deschamps, Precipitation behavior and its effect on strengthening of an HSLA-Nb/Ti steel, Metall. Mater. Trans. A 32(7) (2001) 1635e1647.
[37] L.M. Liu, S.Q. Wang, H.Q. Ye, First-principles study of polar Al/TiN(1 1 1) interfaces, Acta Mater. 52 (12) (2004) 3681e3688.
[38] T.D. Kuhne, T.A. Pascal, E. Kaxiras, Y. Jung, New insights into the structure of the vapor/water interface from large-scale first-principles simulations, J. Phys. Chem. Lett. 2 (2) (2011) 105e113.
[39] C. Zhao, Y. Zhou, X. Xing, S. Liu, X. Ren, Q. Yang, Investigation on the relationship between NbC and wear-resistance of Fe matrix composite coatings with different C contents, Appl. Surf. Sci. 439 (2018) 468e474.

Table 3
Calculated elastic constants C_{ij} of (Nb,M)C.

Phase	C_{11}	C_{12}	C_{13}	C_{33}	C_{44}	C_{66}
NbC	675.18	137.46	137.46	675.18	173.57	173.57
$Nb_{0.75}V_{0.25}C$	653.01	116.28	116.28	653.01	178.13	178.13
$Nb_{0.75}Mo_{0.25}C$	699.79	136.75	136.75	699.79	167.68	167.68
$Nb_{0.75}W_{0.25}C$	739.61	124.52	124.52	739.61	174.03	174.03
$Nb_{0.75}Cr_{0.25}C$	603.07	115.48	115.48	603.07	153.56	153.56

Table 2
Calculated results of lattice constants, elastic modulus, bulk modulus, shear modulus, passion ratio and formation energy.

Phase	Lattice constants	Elastic modulus	Bulk modulus	Shear modulus	Passion ratio	Formation energy
	a(Å)	E(GPa)	B(GPa)	G(GPa)	v	E_{for} (eV/atom)
NbC	4.46	509	316	206	0.23	−0.63
	4.47 [23]	488 [24]	318 [16]	198 [24]	0.22 [24]	−0.71 [25]
$Nb_{0.75}V_{0.25}C$	4.419	509	295	210	0.21	−0.58
$Nb_{0.75}Mo_{0.25}C$	4.426	510	324	206	0.23	−0.48
$Nb_{0.75}W_{0.25}C$	4.434	537	329	219	0.22	−0.44
$Nb_{0.75}Cr_{0.25}C$	4.425	452	278	184	0.22	−0.17

Table 3
Calculated elastic constants C_{ij} of (Nb,M)C.

Phase	C_{11}	C_{12}	C_{13}	C_{33}	C_{44}	C_{66}
NbC	675.18	137.46	137.46	675.18	173.57	173.57
$Nb_{0.75}V_{0.25}C$	653.01	116.28	116.28	653.01	178.13	178.13
$Nb_{0.75}Mo_{0.25}C$	699.79	136.75	136.75	699.79	167.68	167.68
$Nb_{0.75}W_{0.25}C$	739.61	124.52	124.52	739.61	174.03	174.03
$Nb_{0.75}Cr_{0.25}C$	603.07	115.48	115.48	603.07	153.56	153.56

Table 4
Calculated cell volume, Dos at Fermi level, the total number of valance electrons and the metallicity of (Nb,M)C carbides.

Phase	D_f(states/eV)	V_{cell}(Å^3)	N	f_m
NbC	1.90	88.75	68	0.064
$Nb_{0.75}V_{0.25}C$	4.14	86.28	68	0.136
$Nb_{0.75}Mo_{0.25}C$	2.89	86.93	69	0.094
$Nb_{0.75}W_{0.25}C$	2.64	87.21	69	0.086
$Nb_{0.75}Cr_{0.25}C$	3.43	86.69	69	0.112

Table 5
Calculated Mulliken overlap population (MOP): Atomic charges (e) and Bond populations.

		NbC	$Nb_{0.75}V_{0.25}C$	$Nb_{0.75}Mo_{0.25}C$	$Nb_{0.75}W_{0.25}C$	$Nb_{0.75}Cr_{0.25}C$
Atomic populations	C	−0.68	−0.67	−0.65	−0.68	−0.66
			−0.69	−0.68	−0.67	−0.68
	Nb	0.68	0.64	0.75	0.78	0.72
	M		0.80	0.37	0.38	0.49
Bond populations	Nb-C	0.74	0.92	0.69	0.64	0.87
			0.70	0.73	0.73	0.71
	M-C		0.52	0.82	1.03	0.58

Table 6
Adhesion work (J/m^2) and interface distance (Å).

Interface	W_{ad} (J/m^2)		d (Å)	
	M-termination	C-termination	M-termination	C-termination
NbC-Fe	−1.08	0.11	2.88	1.86
NbVC-Fe	1.13	2.02	2.82	1.84
NbMoC-Fe	−2.33	1.40	2.73	1.83
NbWC-Fe	−0.74	−0.71	2.85	1.83
NbCrC-Fe	1.68	3.93	2.80	1.82

Table 7
EDS analysis results of area 1.

Chemical element	area 1	
	Weight percentage	Atom percentage
C	17.01	53.71
Nb	56.65	24.95
Ti	18.93	15.36
V	3.98	3.52
Cr	0.85	0.64
Fe	2.58	1.82

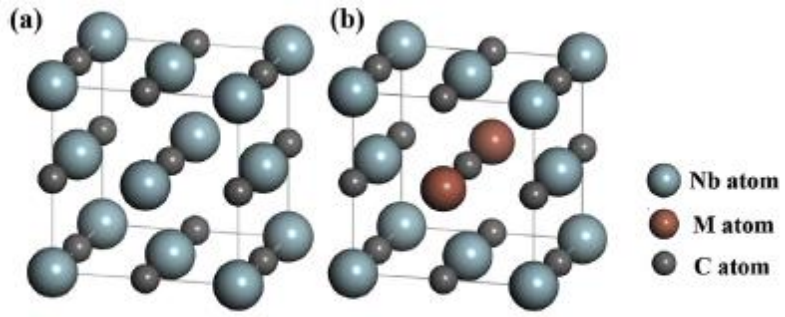

Fig. 1. Structures of NbC and (Nb,M)C.

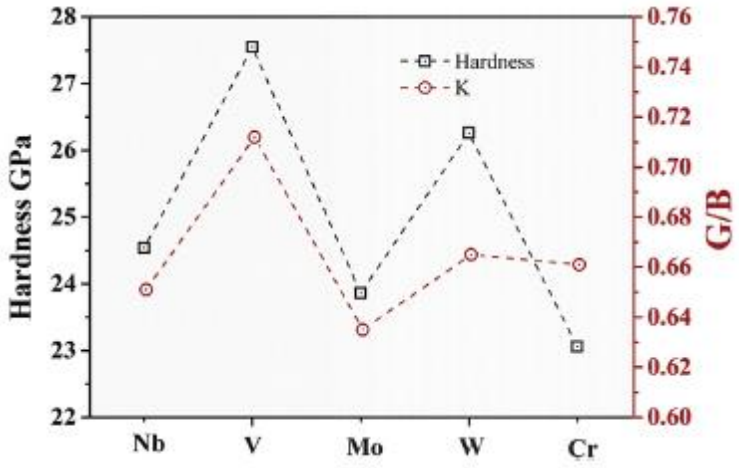

Fig. 2. Theoretical hardness and brittleness of carbides.

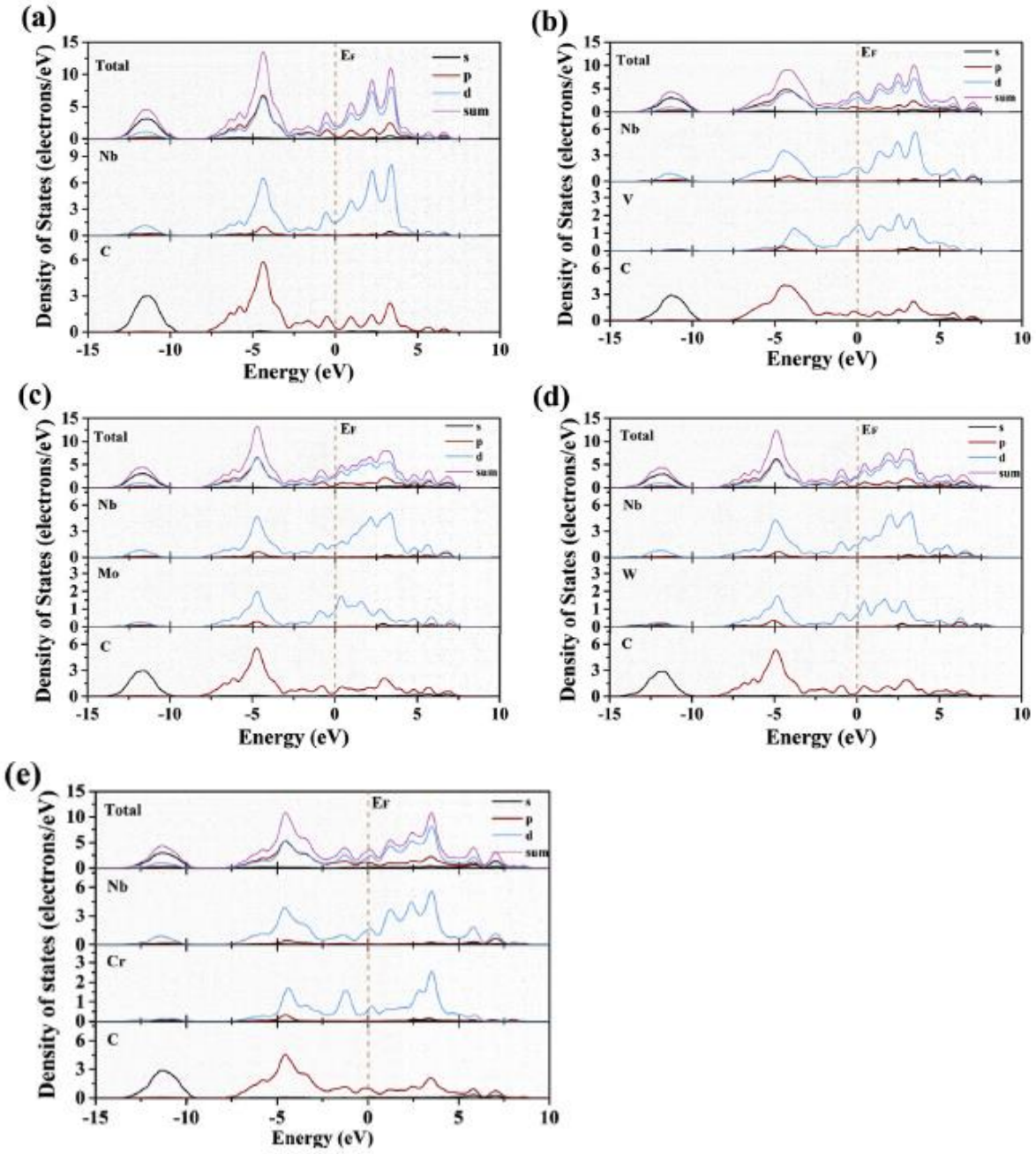

Fig. 3. Total and partial density of state (DOS) for (Nb,M)C: (a) NbC (b) Nb0.75V0.25C (c) Nb0.75Mo0.25C (d) Nb0.75W0.25C (e) Nb0.75Cr0.25C.

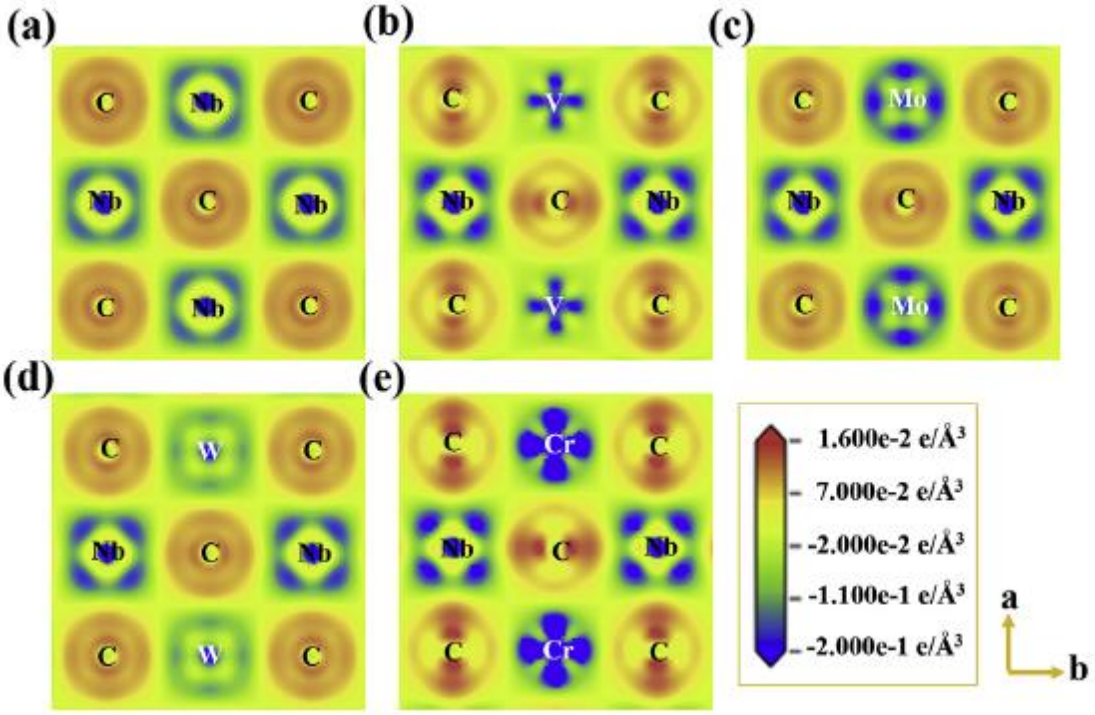

Fig. 4. Charge density difference for Nb0.75M0.25C taken along the (002) plane. (a) NbC (b) Nb0.75V0.25C (c) Nb0.75Mo0.25C (d) Nb0.75W0.25C (e) Nb0.75Cr0.25C.

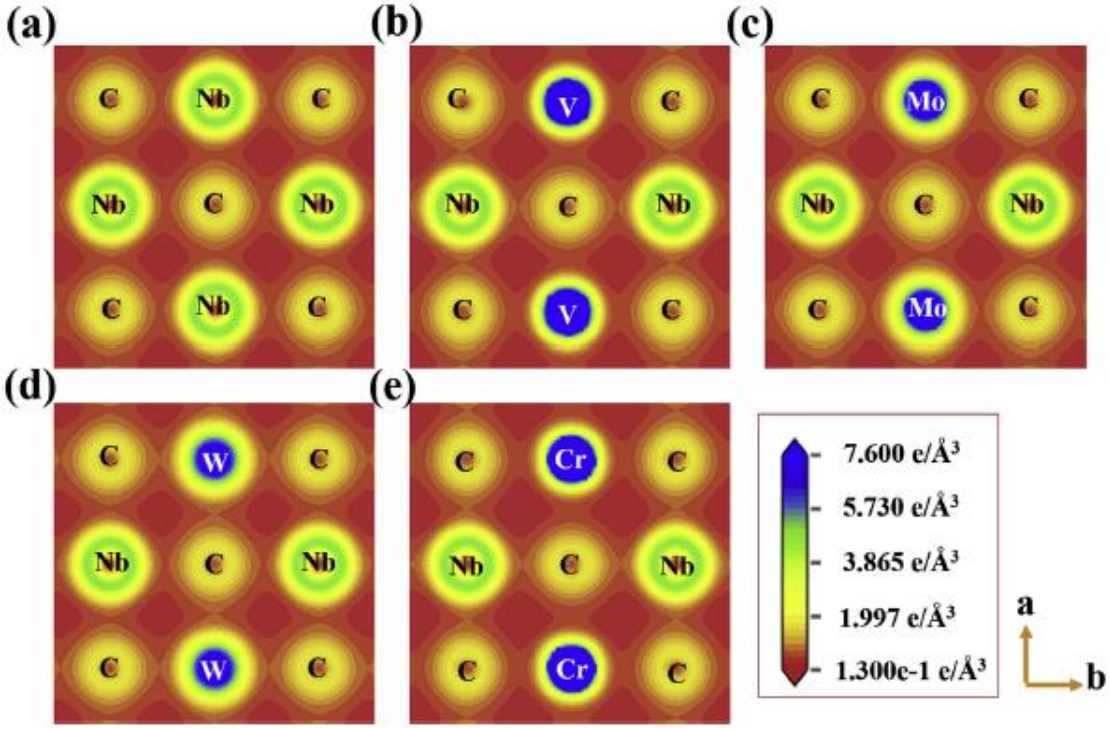

Fig. 5. Charge density for Nb0.75M0.25C taken along the (002) plane. (a) NbC (b) Nb0.75V0.25C (c) Nb0.75Mo0.25C (d) Nb0.75W0.25C (e) Nb0.75Cr0.25C.

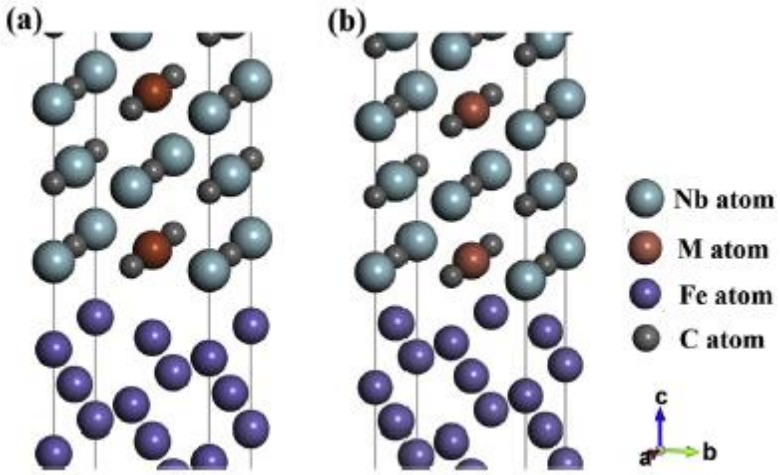

Fig. 6. Interface model of carbide with Fe matrix: (a) metal atoms above the Fe atoms (M-termination) (b) C atoms above the Fe atoms (C-termination).

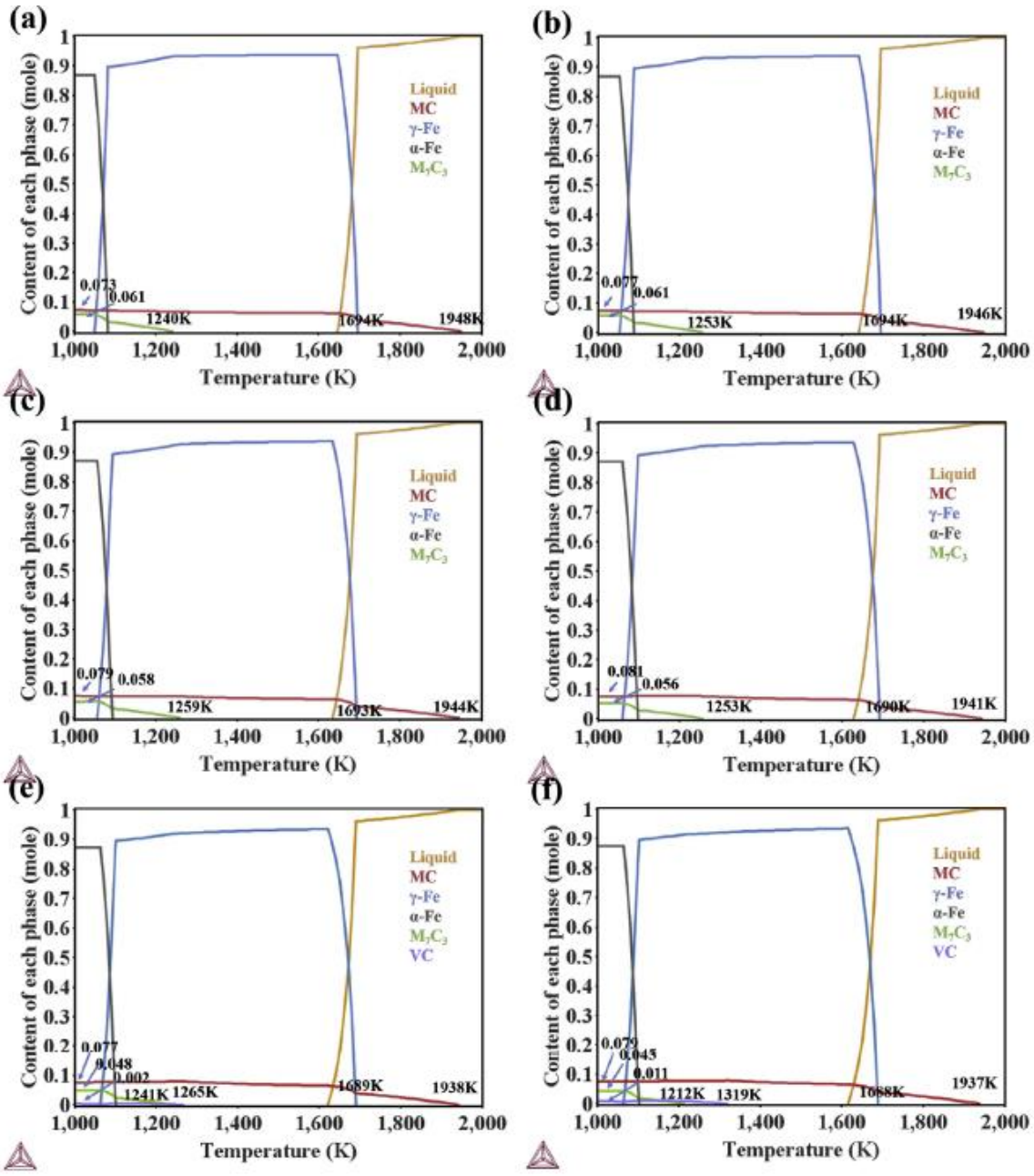

Fig. 7. Diagrams of coatings with different V addition (wt.%): (a) 0 V (b) 0.2 V (c) 0.4 V (d) 0.6 V (e) 0.8 V (f) 1.0 V.

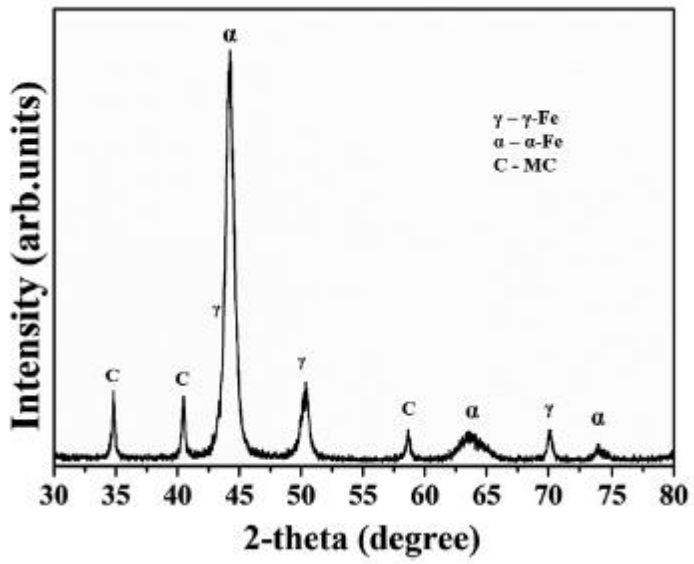

Fig. 8. XRD result of coating.

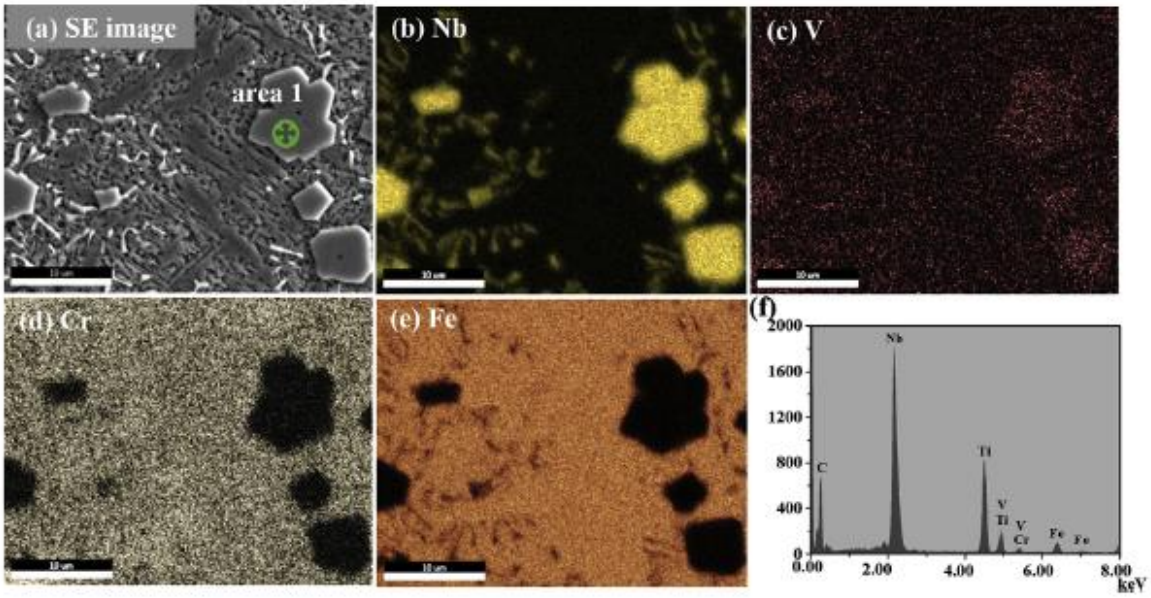

Fig. 9. Morphology and elements mapping of the coatings: (a) SEM image (b) Nb element (c) V element (d) Cr element (e) Fe element (f) EDS results of area 1.

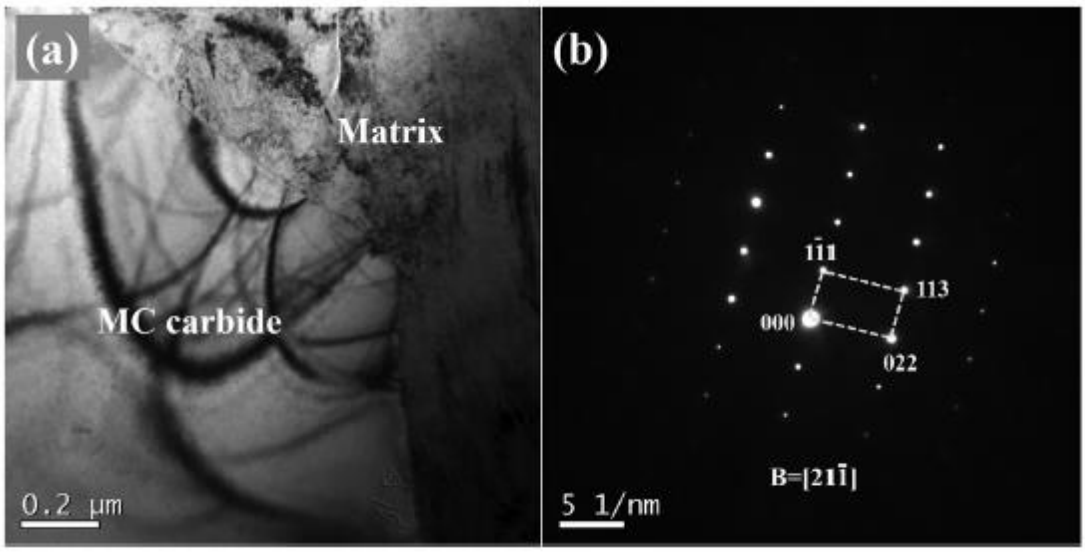

Fig. 10. TEM image of carbide and SEAD pattern of carbide: (a) TEM image (b) SEAD pattern of carbide.